Minería y Geología / v.40 n.1 / enero-marzo / 2024 / p. 25-45 ISSN 1993 8012

ARTÍCULO ORIGINAL

Development and validation of an improved heat transfer calculation model for rough tubes

Desarrollo y validación de un modelo mejorado de cálculo de transferencia de calor para tubos rugosos

Yanan Camaraza-Medina[1]*, Michael Mortensen[2], Yamilka Blanco-Garcia[3]

[1]University of Guanajuato, México.

[2]University of California, Santa Bárbara, USA.

[3]University of Moa, Holguín, Cuba.

*Corresponding author email: ycamaraza1980@gmail.com

Abstract

An improved method for heat transfer calculation inside rough tubes is provided. The model has been obtained from a second assessment developed early by the authors on fluid flow in single-phase inside rough tubes. The proposed correlation has been verified by comparison with a total of 1 666 experimental available data of 34 different fluids, including air, gases, water and organic liquids. The proposal model covers a validity range for Prandtl number ranging from 0.65 to $4.52x10^4$, values of Reynolds number from $2.4x10^3$ to $8.32x10^6$, a range of relative roughness ranging from $5x10^{-2}$ to $2x10^{-6}$ and viscosity ratio from 0.0048 to 181.5. The proposed model provides a good correlation for $10^4 \leq Re$ and $Re < 10^4$, with an average error of 18.3% for 70.4% of the data and 16.6% for 74.8% of the data, respectively. The method presents a satisfactory agreement with the experimental data in each interval evaluated; therefore, the model can be considerate accurate enough for practical application. At the present time, in the available technical literature, a method with similar characteristics is unknown.

Keywords: friction factor; equivalent roughness heat transfer coefficient; average deviation; rough tubes; model.

Resumen

Se presenta un método perfeccionado para el cálculo de la transferencia de calor en el interior de tubos rugosos. El modelo se ha obtenido a partir de una segunda evaluación desarrollada anteriormente por los autores sobre el flujo de fluidos en una sola fase en el interior de tubos rugosos. La correlación propuesta se ha verificado mediante comparación con un total de 1 666 datos experimentales disponibles de 34 fluidos diferentes, entre los que se incluyen aire, gases, agua y líquidos orgánicos. El modelo propuesto cubre un rango de validez para el número de Prandtl que va de 0,65 a 4,52 x 10^4, valores del número de Reynolds de 2,4 x10^3 a 8,32 x10^6, un rango de rugosidad relativa de 5 x10^{-2} a 2 x10^{-6} y una relación de viscosidad de 0,0048 a 181,5. El modelo propuesto proporciona una buena correlación para $10^4 \leq Re$ y $Re < 10^4$, con un error medio del 18,3% para el 70,4% de los datos y del 16,6% para el 74,8% de los datos, respectivamente. El método presenta una concordancia satisfactoria con los datos experimentales en cada intervalo evaluado; por tanto, el modelo puede considerarse suficientemente preciso para su aplicación práctica. Actualmente, en la literatura técnica disponible se desconoce un método con características similares.

Palabras clave: factor de fricción; coeficiente de transferencia de calor de rugosidad equivalente; desviación media; tubos rugosos; modelo.

1. INTRODUCTION

In many industrial processes, to obtain the average heat transfer coefficients is a frequent requirement of energy facilities. For this purpose, due to its simplicity and reasonable approximation, the Dittus-Boelter model is preferred. When the temperature difference is large enough to cause significant changes of viscosity, then the Sieder-Tate model is recommended (Binu and Jayanti 2018; Ataei-Dadavi *et al*. 2019).

The accuracy on the heat transfer prediction can be improved with the use of two models derived from the Prandtl analogy: the equations of Petukhov (1970) and Gnielinski (2013) for $(10^4 \leq Re \leq 5 \times 10^6)$ and $(3 \times 10^3 \leq Re \leq 5 \times 10^6)$, respectively (Reis *et al*. 2018). Recently, a new model that shows a satisfactory fit was proposed; with validity range $2.3 \times 10^3 \leq Re \leq 8.2 \times 10^6$ (Camaraza-Medina, Cruz-Fonticiella and García-Morales 2019).

In heat transfer equipment, tubes generally have a low surface roughness, therefore, in calculations they are considered as smooth $e/d \approx 0$. However, the continued use increases gradually the aging and surface roughness of the tubes, which exerts a notable effect on the fluid circulation, and therefore, on the average heat transfer coefficient. The dimensionless roughness is a widely used term that establishes the roughness pattern, and is given by Equation (1) (Chen *et al*. 2019):

$$C = \mathrm{Re} \cdot e/d \cdot \sqrt{f/8} \quad (1)$$

In Equation (1), $e/d$is the relative roughness; $Re$is the Reynolds number and $f$is the Darcy friction factor.

Nomenclature

B	Constant defined in Equation (5)	Pr	Prandtl number
C	Dimensional roughness (Equation (1))	Re	Reynolds number
D	Constant defined in Equation (3)	Re_m	Modified Reynolds number
D_{mean}	Percentage of data that correlates under *MAE* values	T_F	Average fluid temperature, ˚C
$D_{\%}$	Deviation percent, defined in Equation (7)	T_P	Wall temperature, ˚C
E	Modified Prandtl number, defined in Equation (5)		
E_{max}	Maximum error		**Greek symbols**
MAE	Mean absolute error, %		
e/d	Relative roughness	α_R	Heat transfer coefficient, kg·m^{-1}·K^{-1}·s^{-1}
f	Darcy friction factor	α_{exp}	Experimental heat transfer coefficient, kg·m^{-1}·K^{-1}·s^{-1}
N	Constant defined in Equation (5)	μ_F	Fluid dynamic viscosity at T_F, kg·m^{-1}·s^{-1}
Nu	Nusselt number	μ_P	Fluid dynamic viscosity at T_P, kg·m^{-1}·s^{-1}

When $C \leq 5$, the surface roughness has a negligible influence on the average heat transfer coefficient. However, for $C > 5$, the surface roughness has a significant influence, therefore, in the heat transfer calculations it must be considered (Bazán, Bedin and Bozzoli 2016; Rabiee *et al*. 2018).

In the technical literature, several works that describe comparisons between available models are found; however, these do not consider the effect of the friction factor on the average heat transfer coefficient. Models derived from the Prandtl analogy and logarithmic adjustments as Petukhov (1970), Gnielisnky (2013) and Camaraza *et al.* (2020) respectively, include this effect, but only for $C \leq 5$ (Camaraza-Medina, Hernandez-Guerrero and Luviano-Ortiz 2020).

During the 1990's, some works focused on improving the correlation indexes in the available correlations offering an approximate techniques for models derived from the Prandtl analogy (for this purpose, the friction factor may be determined with the help of the Moody chart) however, these models do not provide satisfactory results, because in tests carried out, mean absolute error (*MAE*) of ±30% and maximum errors (E_{max}) near 80% have been found (Camaraza-Medina *et al*. 2019a). For heat transfer calculations during fluid

flow in single-phase inside rough tubes, in the literature several correlations are found; however, only a reduced range of relative roughness is considered in these correlations (Song, Cui and Liu 2017).

An important research focused on transition and turbulent flow was made by Bhatti-Shah (Bhatti and Shah 1987). In this work, the influence of a turbulence dimensionless parameter (turbulent Prandtl number) is considered, allowing to extend the validity range of the model and improving the accuracy of the heat transfer calculations. Similarly, a corrective term to consider the influence of dimensionless roughness on the mean coefficient was included. This correlation has a mean deviation of 20% with respect to the available experimental values and is suitable for $C > 5$.

Recently, one model for improving the heat transfer calculations in rough tubes was developed. This correlation has a mean deviation of 18% with respect to the available experimental values and increases the validity range and the friction factor is estimated by means of a procedure for non-isothermal conditions (Medina, Fonticiella y Morales 2017, Camaraza-Medina *et al*. 2019b).

Currently, in the available literature there exists no study that provides *MAE* and E_{max} variations for the existing models, neither, the number of data that complies with a acceptable *MAE* values. For this purpose, in the present work, a total of 1 666 experimental data of 34 different fluids were compiled, including air, gases, water and organic liquids. Available experimental data were correlated with three known models in the literature, Bhatti-Shah, Gnielinski and the modified Gnielinski method (using Moody chart for the friction factor). A summary of the equations used and their validity range is given by Song, Cui and Liu (2017).

To develop a correlation for heat transfer calculation inside rough pipes, with a larger validity range with respect to known models, while providing lower indexes of *MAE* and E_{max} is the main objective of the present paper. Additionally, a description and tabulation of the main results using the correlation of the selected models and also the correlation proposed in the present work with available experimental data is offered as well.

2. METHODS AND VALIDATION

2.1. Development of the proposed model

The Prandtl model is taken in this research as a starting point, which is provided by Camaraza-Medina *et al*. (2020):

$$Nu = \frac{f}{8} \cdot Re \cdot Pr \cdot \left[1 + 5 \cdot \sqrt{\frac{f}{8}} \cdot (Pr - 1)\right]^{-1} \quad (2)$$

Equation (2) is suitable for turbulent flow $(10^4 \leq \mathrm{Re})$, however, for transition flow $(2.4 \times 10^3 \leq Re < 10^4)$, the modified Reynolds is required. In this paper, the modified Reynolds is provided by:

$$Re_m = (Re - 10^D) \tag{3}$$

In Equation (3), the exponent *D* has a logarithmic dependence, obtained by adjusting the experimental data (Figure 1). A regression analysis shows that the exponent *D* is given by:

$$D = (-0.76 \cdot \ln f + 2.43) \cdot f^{0.15} \tag{4}$$

In Equation (4) f is the Darcy friction factor, which is obtained according to recommendations provided in Mondal and Field (2018).

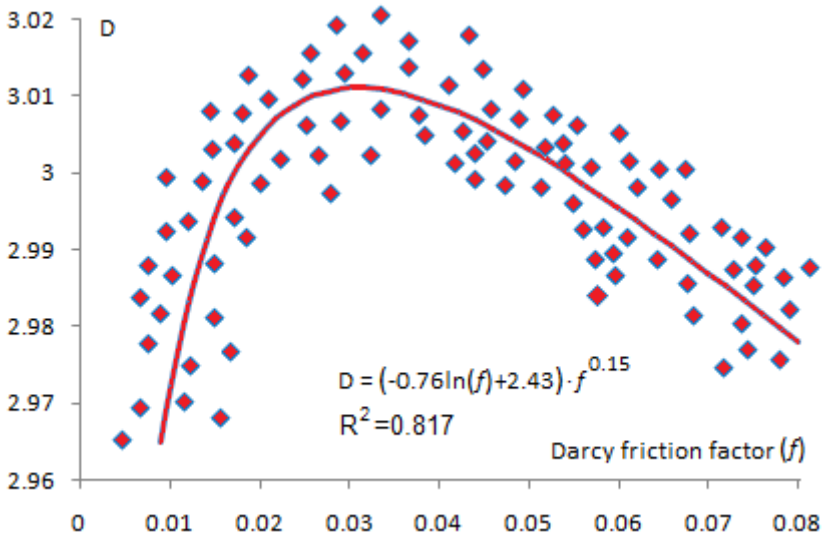

Figura 1. Experimental data correlation with the Equation (4).

The experimental data used in the validation of the selected model were extracted from Medina *et al.* (2018) and summarized in Table 1, which presents a comparison of the proposed correlation with a wide range of experimental data.

Table 1. Comparison of equation (5) and available experimental data

Source	Number of data	Fluid	e/d	$Re \times 10^3$	Pr	μ_F/μ_P	Deviation percent
Milman (1973)	34	Air	0.001	14	0.68	0.64	14.6
			0.005	4810	0.7	1.66	-12.3
Rosson (1955)	29	Turpentine	0.001	13	14.3	0.41	10.7
			0.005	109	29.8	2.43	-14.9
Borishanskiy *et al*. (1973)	27	Water	0.04	98	1.2	0.24	13.4
			0.006	262	6.0	0.86	-9.1
	28	Pentane	0.005	135	4.5	0.47	16.1

			0.0001	619	7.2	2.08	-19,6
	23	Transformeroil	0.025	3.1	32.1	0.012	20.1
			0.001	10.3	1490	114.1	-16,7
Houng *et al*. (2019)	49	Water	0.04	7.2	1.9	0.19	14.3
			0.000	620	10.6	5.1	-11.8
	31	Ethyl iodide	0.03	12.3	3.6	0.53	9.2
			0.001	31.4	5.3	1.87	-10.4
	33	Transformer oil	0.01	3.9	45	0.02	15.3
			0.008	10.1	1510	110.4	-17.1
Boyko (1965)	42	Water	0.008	13.8	2	0.18	18.6
			0.0005	540	12	3.15	-13.9
Andreijin *et al*. (1965)	26	Benzene	0.001	2.5	3.1	0.3	18.9
			0.0005	20.2	5	3.18	-7.6
Camaraza *et al* (2018)	38	Water	0.02	280	0.93	0.19	15.3
			0.004	2200	11	3.96	-17.9
Efimok (1967)	42	Nitrogen	0.01	6	0.68	0.15	19.8
			0.005	8100	0.75	6.5	-11.9
I'lin (1950)	38	Air	0.05	7	0.68	0.65	16.3
			0.01	5100	0.7	1.65	-10.5
Kirilov (1969)	49	Carbondioxide	0.01	14	0.66	0.3	7.2
			0.005	660	0.81	3.3	-10.7
Vukalovich (1963)	21	Air	0.01	12.5	0.68	0.65	17.2
			0.005	3700	0.7	1.65	-10.5
Sabersky (1962)	32	Water	0.05	25	1	0.13	14.1
			0.01	180	9.44	7.15	-5.9
	44	Helium	0.02	9	0.71	0.22	17.1
			0.005	40	0.72	4.5	-12.3
Osipova (1964)	47	Isobutene	0.01	1200	0,73	0.68	19.7
			0.005	5200	0,75	1.46	-16.4
	28	Water	0.0001	18	0.9	0.19	16.2
			0.0005	550	9.4	0.77	-10.9
	46	Methylformate	0.04	12.6	3.7	0.38	7.1
			0.001	245.1	7.0	2.63	-4.2
Amoroz *et al*. (2019)	56	Water	0.05	980	1	0.1	9.3
			0.0001	8250	11.1	10.1	-12.4
	47	Water	0.015	970	1.2	0.13	10.4
			0.0005	8320	10.4	7.48	-13.1
	109	Water	0.05	450	2.3	0.3	14.3

			0.000002	7850	9.2	3.6	-16.1
Aljamal*et al*. (2018)	43	Gasoline	0.05	70	5.8	0.38	9.4
			0.0001	6900	11.0	2.62	-11.4
	21	Transformer oil	0.008	3.2	33.9	0.01	19.3
			0.0001	10.8	1540	115.2	-14.3
	29	Glycerin	0.04	2.4	1620	0.018	19.2
			0.01	9.0	22150	55,4	-15.4
Akers *et al.* (1970)	14	MC oil	0.03	5	120	0,07	14.8
			0.001	10.4	9800	133,3	-17.1
	19	MK oil	0.008	5.2	580	0.011	14.8
			0.0001	8.6	38200	88.7	-11.6
Dipprey (1967)	12	Butyl alcohol	0.03	40	23	0.08	14.3
				75	30	0.45	-12.2
Dorsch (1969)	23	Gasoline	0.05	70	5.5	0.22	10.4
			0.015	6900	15.1	4.4	-6,1
	23	Hydrogen	0.004	12	0.65	0.48	12.4
			0.0001	8200	0.73	3.28	-10.8
Camaraza *et al*. (2019)	41	Water	0.004	4	2.2	0.27	10.9
			0.0001	200	9.4	3.68	-11.5
Karkalala (2012)	54	Water	0.002	1200	1.2	0.24	5.3
			0.005	2800	5.9	0.96	-4.5
Mudawar *et al*. (2017)	30	Engine Oil	0.03	2.4	318.8	0.0056	19.1
			0.0001	10.1	45200	181.5	-21.4
Carpenter (1957)	19	Methanol	0.001	2.9	2.2	0.1	9.4
			0.00005	1112.1	7.7	9.9	-12.1
Vasserman (1962)	22	Kerosene	0.03	6.4	1.35	0.38	10.1
			0.005	52.8	2.9	2.6	-2.3
	19	Acetic acid	0.03	3.0	8.5	0.8	4.7
			0.005	988	14.2	1.2	-13.7
	28	Acetaldehyde	0.03	3.9	2.85	0.4	8.2
			0.005	52.4	4.4	2.1	-7.9
	31	Butanol	0.03	5.4	22.5	0.04	11.6
			0.005	102.6	3860	24.6	-16.7
	17	Aniline	0.03	4.4	11.5	0.08	9.7
			0.005	1020	111	12.35	-13.5
	15	Carbon disulfide	0.03	13.7	2.3	0.59	11.2
			0.005	76.6	3.2	1.68	-10.1

Jung *et al*. (2015)	13	Ciclohexane	0.03 0.005	36.2 89.3	11 19.9	0.5 1.9	12.3 -16.7
	23	Transformer oil	0.01 0.0015	2.8 8.6	34.9 4800	1.2 28.3	16.2 -17.5
	23	Ethanol	0.04 0.01	21.4 1514	6.9 68.4	0.049 20.5	7.2 -8.4
	28	Ethyl ether	0.007 0.0001	520 2480	3.5 7.3	0.3 3.6	6.2 -10.1
	27	Ethylamine	0.008 0.0001	12.1 17.8	5.1 8.3	0.55 1.8	3.2 -6.1
	31	Propylene	0.04 0.01	125 284	2.8 3.2	0.27 3.66	9.1 -4.8
Mortensen (2019)	28	Dodecane	0.04 0.025	72 96	10.7 28.2	0.4 3.3	11.1 -12.4
	17	Decane	0.05 0.015	16 47.2	6.8 17.1	0.25 4.1	6.3 -7.8
	19	Ethyleneglycol	0.01 0.02	6.3 12.1	69 510	0.12 8.1	17.1 -19.3
	41	Methanol	0.015 0.0001	8.7 234.5	5.9 15.1	0.32 3.1	8.2 -4.3
	37	Ethanol	0.05 0.001	9.2 106.8	13 52.5	0.17 5.73	13.4 -16.2
For all sources above	1666		0.05 0.000002	2.4 8320	0.65 45200	0.0048 181.5	20.1 -21.4

The proposed correlation was obtained by means of a modeling process, applying superposition variables techniques on Equation (2) (Cancan *et al*. 2017; Shankar and Senadheera 2024). Adjustment and validation of the available experimental data allowed obtaining the new correlation, given by:

$$\mathrm{Nu} = \frac{\mathrm{f}\cdot\left(\mathrm{Re}-10^{\mathrm{D}}\right)\cdot\mathrm{Pr}}{8+(1.265-\mathrm{E}^{0.8})\cdot\mathrm{B}-\sqrt{576\cdot\mathrm{f}}}\cdot\left(\frac{\mu_{\mathrm{F}}}{\mu_{\mathrm{P}}}\right)^{\mathrm{N}} \quad (5)$$

The constant Nused in Equation (5) takes values 0.25 and 0.11 for fluid cooling or heating, respectively; E is the modified Prandtl number (Table 2); B is a constant value defined by Equation (6):

$$\mathrm{B} = 31.635\cdot(\mathrm{Re}\cdot e/d)^{0.2}\cdot\mathrm{f}^{0.6}\cdot\sqrt{\mathrm{Pr}} \quad (6)$$

Table 2**.** Values of modified Prandtl number

Zone	Validity range	Value of constant E
1	$0.6 \leq \mathrm{Pr} < 140$	$\mathrm{E} = 0.84 - 0.076 \cdot (\log \mathrm{Pr})^2$
2	$140 \leq \mathrm{Pr} < 1.72 \times 10^3$	$\mathrm{E} = 0.95 - 0.25 \cdot (\log \mathrm{Pr})^{0.94}$
3	$1.7 \times 10^3 \leq Pr$	$\mathrm{E} = 0.92 - 0.44 \cdot (\log \mathrm{Pr})^{0.43}$

Equation (5) is applicable in tubes if $\mathrm{C} > 5$.When $\mathrm{C} \leq 5$, heat transfer coefficient can be obtained by means of the smooth tubes criteria (Petukhov or Gnielinski). The dimensional roughness C is described by Equation (1) (Huang *et al*. 2016).

Figures 2 to 4 show the correlation between the experimental data and the models summarized in Table 2. Table 3 provides a detailed summary of the validity range, showing a satisfactory fit with Equation (5).

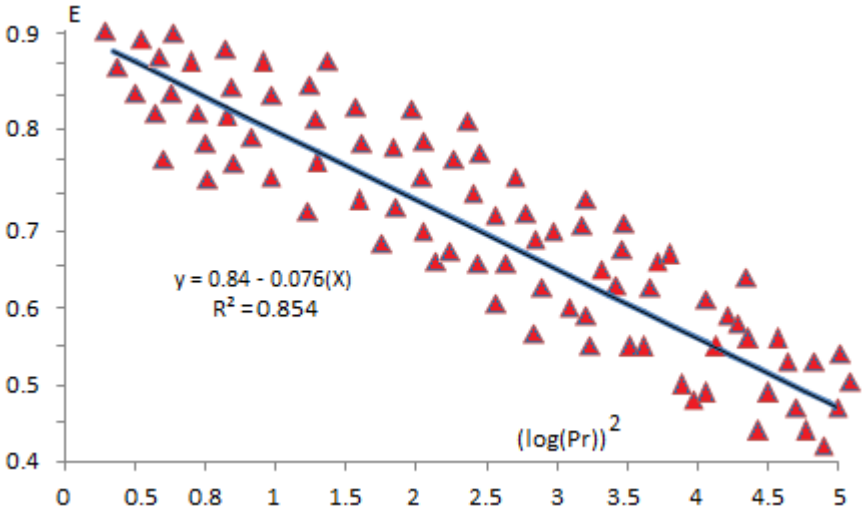

Figura 2. Functional adjustment of values E in Zone 1.

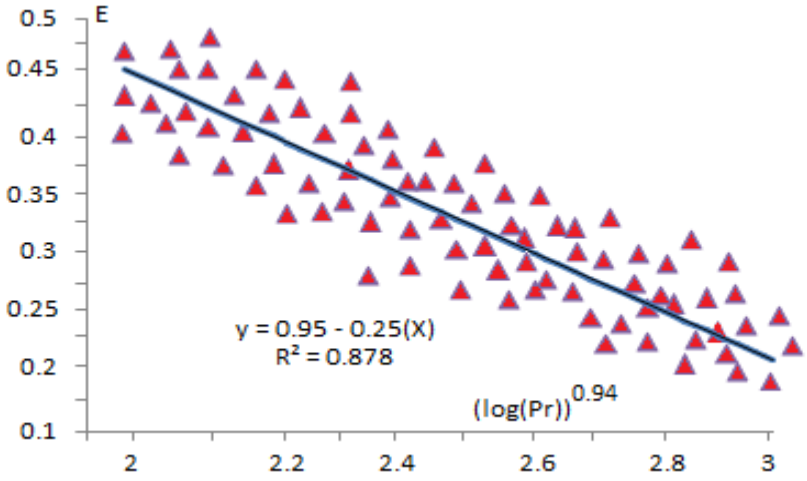

Figura 3. Functional adjustment of values E in Zone 2.

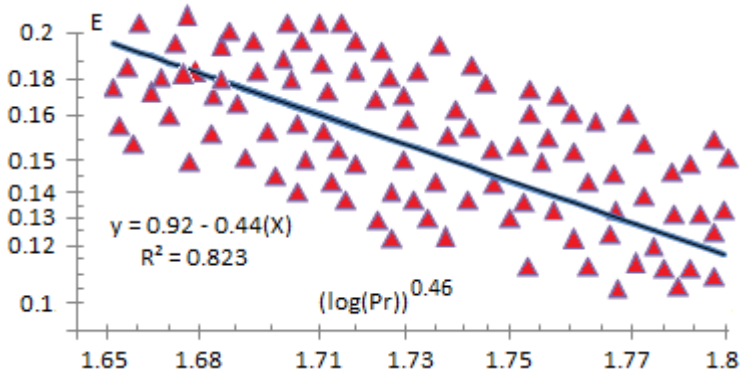

Figura 4. Functional adjustment of values E in Zone 3.

Tables 4 and 5 show the comparison between Equation (5) and the experimental data, for transitional and turbulent regime respectively, dividing into eight subintervals the validity range.

Table 3**.** Summary of validity range for equation (5)

Parameter	**Range**
Fluids	Acetaldehyde, Acetic acid, Air, Aniline, Benzene, Butanol, Butyl alcohol, Carbon dioxide, Carbon disulfide, Ciclohexane, Decane, Dodecane, Engine oil, Ethanol, Ethyl ether, Ethyl iodide, Ethylamine, Ethylene glycol, Gasoline, Glycerin, Helium, Hydrogen, Isobutene, Kerosene, MC oil, Methanol, Methyl formate, MK oil, Nitrogen, Pentane, Propylene, Transformer oil, Turpentine and Water.
Pr	0.65 to 4.52×10^4
Re	2.4×10^3 to 8.32×10^6
μ_F/μ_P	$0.0048 \leq \mu_F/\mu_P \leq 181.5$
e/d	$5 \times 10^{-2} \leq e/d \leq 2 \times 10^{-6}$
C	$C > 5$

Table 4. Comparison between Equation (5) and experimental data for transitional regime

$2.4 \times 10^3 \leq Re < 10^4$		
$0.0048 < \frac{\mu_F}{\mu_P} \leq 10$	$0.05 \leq e/d \leq 10^{-3}$	$error < 11.1\%$ 84.5% data
$0.0048 < \frac{\mu_F}{\mu_P} \leq 19.1$	$0.05 \leq e/d \leq 8 \times 10^{-4}$	$error < 11.9\%$ 83.2% data
$0.0048 < \frac{\mu_F}{\mu_P} \leq 25.7$	$0.05 \leq e/d \leq 4 \times 10^{-4}$	$error < 12.7\%$ 81.8% data
$0.0048 < \frac{\mu_F}{\mu_P} \leq 39.4$	$0.05 \leq e/d \leq 2 \times 10^{-4}$	$error < 13.2\%$ 79.7% data
$0.0048 < \frac{\mu_F}{\mu_P} \leq 68.5$	$0.05 \leq e/d \leq 8 \times 10^{-5}$	$error < 13.9\%$ 78.6% data

$0.0048 < \frac{\mu_F}{\mu_P} \leq 100$	$0.05 \leq e/d \leq 4 \times 10^{-5}$	$error < 14.3\%$ 76.5% data
$0.0048 < \frac{\mu_F}{\mu_P} \leq 140$	$0.05 \leq e/d \leq 2 \times 10^{-5}$	$error < 15.1\%$ 75.7% data
$0.0048 < \frac{\mu_F}{\mu_P} \leq 181.5$	$0.05 \leq e/d \leq 2 \times 10^{-6}$	$error < 16.6\%$ 74.8% data

Table 5**.** Comparison between Equation (5) and experimental data for turbulent regime

$10^4 \leq Re \leq 8.32 \times 10^6$		
$0.0048 < \frac{\mu_F}{\mu_P} \leq 10$	$0.05 \leq e/d \leq 10^{-3}$	$error < 11.8\%$ 80.2% data
$0.0048 < \frac{\mu_F}{\mu_P} \leq 19.1$	$0.05 \leq e/d \leq 8 \times 10^{-4}$	$error < 12.6\%$ 79.3% data
$0.0048 < \frac{\mu_F}{\mu_P} \leq 25.7$	$0.05 \leq e/d \leq 4 \times 10^{-4}$	$error < 13.8\%$ 77.9% data
$0.0048 < \frac{\mu_F}{\mu_P} \leq 39.4$	$0.05 \leq e/d \leq 2 \times 10^{-4}$	$error < 15.1\%$ 76.2% data
$0.0048 < \frac{\mu_F}{\mu_P} \leq 68.5$	$0.05 \leq e/d \leq 8 \times 10^{-5}$	$error < 15.9\%$ 75.1% data
$0.0048 < \frac{\mu_F}{\mu_P} \leq 100$	$0.05 \leq e/d \leq 4 \times 10^{-5}$	$error < 16.7\%$ 73.4% data
$0.0048 < \frac{\mu_F}{\mu_P} \leq 140$	$0.05 \leq e/d \leq 2 \times 10^{-5}$	$error < 17.8\%$ 71.8% data
$0.0048 < \frac{\mu_F}{\mu_P} \leq 181.5$	$0.05 \leq e/d \leq 2 \times 10^{-6}$	$error < 18.3\%$ 70.4% data

3. ANALYSIS OF RESULTS

3.1. Required element for the comparative study

In the examined correlations, the model proposed in this work has the larger validity range, therefore, to execute a comparative study, its validity range is divided in eight sub-intervals, summarized in Tables 4 and 5. The deviation percent (error) is computed with respect to the proposed correlation and is provided by Bae, Kim and Chung (2018):

$$D_{\%} = 100 \cdot \left(\frac{\alpha_R - \alpha_{exp}}{\alpha_R}\right) \quad (7)$$

In Equation (7) $D_{\%}$ is the deviation percent, α_R and α_{exp} are the heat transfer coefficients obtained with Equation (5) and experimentally, respectively.

The mean absolute error (*MAE*) is calculated as Thomas *et al*. (2024):

$$MAE = \frac{1}{n}\sum_n \left|\frac{\alpha_R - \alpha_{exp}}{\alpha_R}\right| \quad (8)$$

In Equation (8) n is the number of experimental data available. In order to accomplish this correlation study, the experimental available data were separated in two groups (Table 6), for turbulent and transition zones.

The study was carried out with 1 666 experimental data. In Table 6, the N values of experimental data available for each validity range of the model are summarized, in agreement with the classification given in Tables 4 and 5.

The experimental data available are grouped in the eight intervals given in Tables 4 and 5 and thus the data of each zone with the four models selected for this study are correlated, obtaining for each model the percentage values of data that correlates under *MAE* values (D_{mean}),the maximum error (E_{max}) and the *MAE* values.

Table 6**.** Summary of the n values used by intervals

Interval	$\mathbf{2.3 \times 10^4 \leq Re < 10^4}$	$\mathbf{10^4 \leq Re < 8.2 \times 10^6}$
1	207	482
2	266	615
3	307	708
4	354	784
5	377	843
6	391	938
7	412	1043
8	437	1229

3.2. Summary of the main results obtained in the evaluation of the transition zone

In Figures 5 to 7, the values of E_{max}, *MAE* and D_{mean} obtained in the correlation developed between selected models and available experimental data are given in graphical form.

The study shows that in the transition zone, the fundamentals results used in the comparison concentrate on three fundamental elements, described early ($E_{\max}$, $D_{\text{mean}}$and *MAE*). In these, for $2.4 \times 10^3 \leq Re < 10^4$, it is confirmed that the model proposed in the present work has the best *MAE* adjustment values, showing an average error of 11.1 % and 16.6 %, for 84.5 % and 74.8 % of the available data for Intervals 1 and 8, respectively.

In the specialized literature (Shankar and Senadheera 2024) it is established that Bhatti-Shah's model correlates with an average error of 15 %; however, the results obtained in the present study show an average error of 13.5 %

and 18.4 % for 81.6 % and 70.3 % of the data for Intervals 1 and 8, respectively, proving that the values obtained in the present study are slightly higher to the values commonly attributed in the literature.

The most unfavorable indicators are obtained using the models of Gnielinski, which provide *MAE* values of 23.2 % and 32.8 % for 72.5 % and 60.1 %, respectively of the experimental data, for Intervals 1 and 8, which agrees well with those results given by Shankar and Senadheera (2024).

The modified correlation of Gnielinski provides fairly acceptable adjustments of correlation, with *MAE* values of 18.9 and 25.9 % for 74.8 % and 62.9 % of the experimental data, respectively for Intervals 1 and 8; this indicates that Gnielinski's model can be used for a rapid estimation of the heat transfer coefficients in the transition zone, which confirms the recommendations given by Thomas *et al*. (2024).

Equation (5) and Bhatti-Shah's model, show the best D_{mean}index, with 84.5 % and 81.6 %, respectively, in Interval 1, while these values decrease to 74.8 % and 70.3 % for Interval 8. On the contrary, the modified correlation of Gnielinski and the Gnielinski's model, have the most unfavorable indexes, with 74.8 % and 72.5 % respectively in Interval 1, decreasing to 62.9 % and 60.1 % for Interval 8.

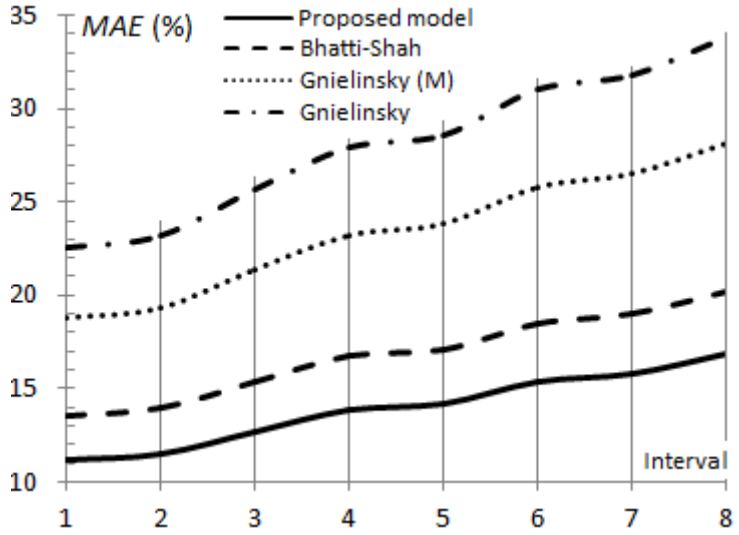

Figura 5. *MAE* values in the correlation data (transition zone).

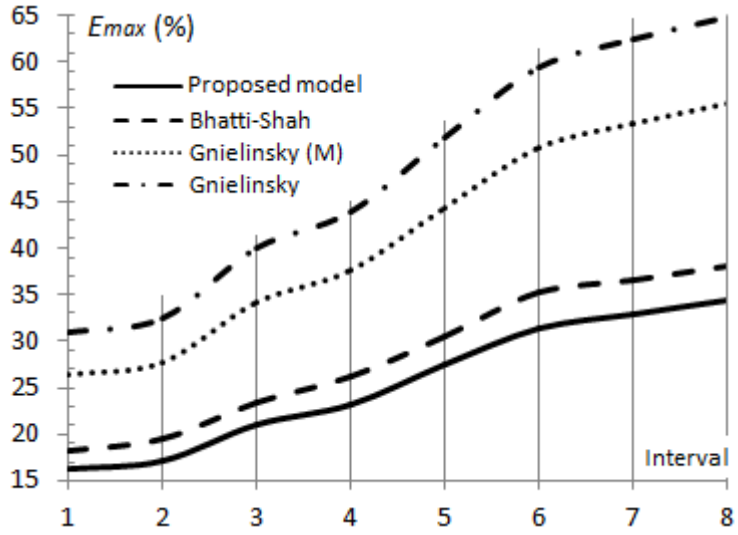

Figura 6. E_{max} values in the correlation data (transition zone).

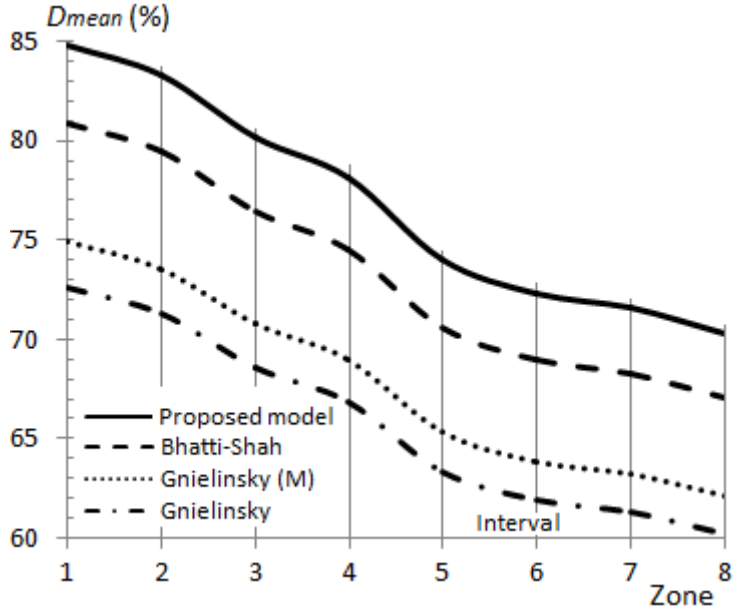

Figura 7. D_{mean} values in the correlation data (transition zone).

The known technical literature does not contain recommendations that suggest the maximum error with the use of a determined model. In the present research, values of E_{max}generated with the use of every model for the eight studied intervals was obtained. For this purpose, a comparison between available experimental data and the selected models was made.

Equation (5) and Bhatti-Shah's model show the best $E_{\max}$ index, with 16.9 % and 19.1 % respectively in Interval 1, while these values increase to 32.3 % and 36.5 % for Interval 8. On the contrary, the more unfavorable indexes are obtained with the modified correlation of Gnielinski and Gnielinski's model, which provide $E_{\max}$ values of 27.3 % and 31.4 % respectively for Interval 1, increasing to 54.7 % and 64.8 % in Interval 8.

Based on the results of this study, it is confirmed that the modified correlation of Gnielinski can be used reservedly to determine the heat transfer coefficients in the transition regime, being preferable not to extend their use beyond Interval 1.

3.3. Summary of the main results obtained in the evaluation of the turbulent zone

In Figures 8 to 10, the values of E_{max}, *MAE* and D_{mean}obtained in the correlation developed between the selected models and the available experimental data are given in graphical form.

The study shows that in the turbulent zone, the main results used in the comparison concentrate on three fundamental elements, described early ($E_{\max}$, D_{mean} and *MAE*). In these, for $10^4 \leq Re < 8.2 \times 10^6$, it is confirmed that Equation (5) have the best *MAE* adjustment values, showing an average error of 11.8 % and 18.3 % for 80.2 % and 70.4 % of the available data for Intervals 1 and 8, respectively.

In the specialized literature it is established that Bhatti-Shah's model correlates with an average error of 10 % and 15 % for Intervals 1 and 8 respectively; however, the results obtained in the present study show an average error of 13.8 % and 18.6 % for 77.9 % and 68.1 % of the data for Intervals 1 and 8, respectively, proving that the values obtained in the present study are slightly higher to the values commonly attributed in the literature.

The most unfavorable indicators are obtained using the model of Gnielinski, which provide *MAE* values respectively of 23.9 % and 36.6 % for 67.1 % and 56.8 % of the experimental data, respectively for Intervals 1 and 8, which agrees well with those results given by Thomas *et al*. (2024).

Equation (5) and Bhatti-Shah's model show the best D_{mean}index, with 80.2 % and 77.9 % respectively in Interval 1, while these values decrease to 70.4 % and 68.1 % for Interval 8. On the contrary, the modified correlation of Gnielinski and the Gnielinski's model, have the most unfavorable indexes, with 70.2 % and 67.1 % respectively in Interval 1, decreasing to 60.4 % and 56.8 % for Interval 8.

Equation (5) and Bhatti-Shah's model show the best $E_{\max}$ index, with 17.3 % and 20.1 % respectively in Interval 1, while these values increase to 34.1 % and 39.7 % for Interval 8. On the contrary, the most unfavorable indicators are obtained with the modified correlation of Gnielinski and Gnielinski's model, which provide $E_{\max}$ values of 28.7 % and 34.6 % respectively for Interval 1, increasing to 56.8 % and 68.9 % in Interval 8.

The modified correlation of Gnielinski provides fairly acceptable adjustments of correlation, with *MAE* values of 19.2 % and 28.4 % for 70.2 % and 60.4 % of the experimental data, respectively for Intervals 1 and 8; this indicates that it can be used for a rapid estimation of the heat transfer coefficients in the turbulent zone, which confirms the recommendations given by Medina *et al*. (2017):

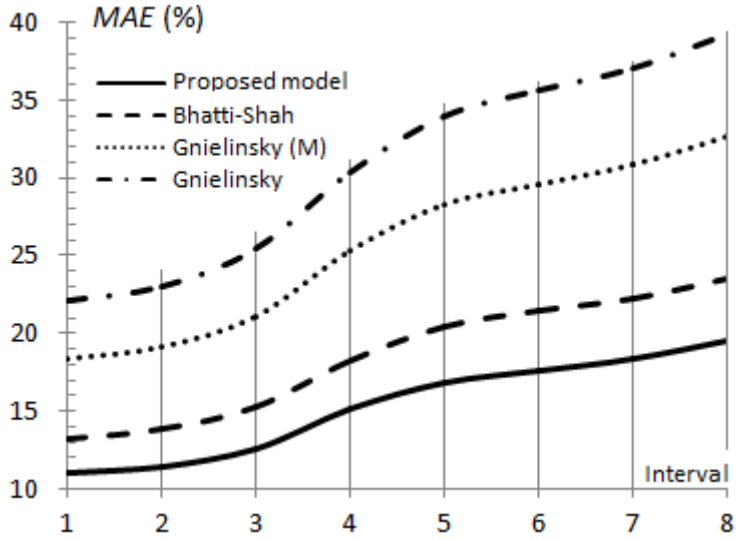

Figura 8. *MAE* values in the correlation data (turbulent zone).

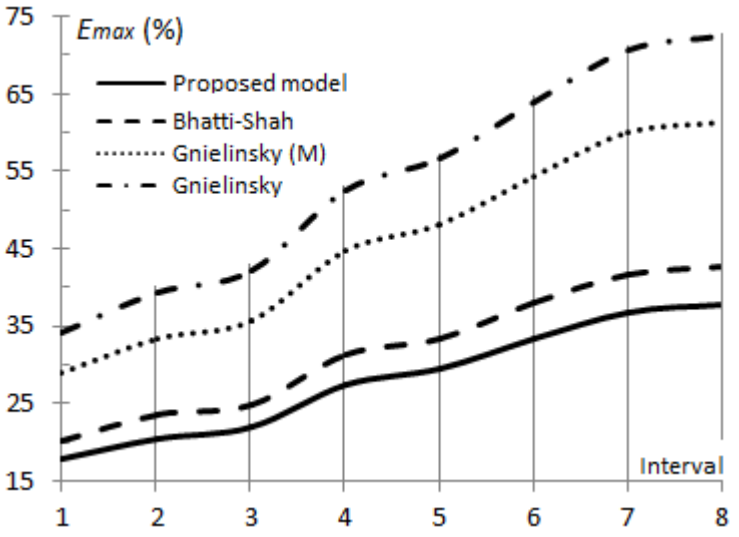

Figura 9. E_{max}values in the correlation data (turbulent zone).

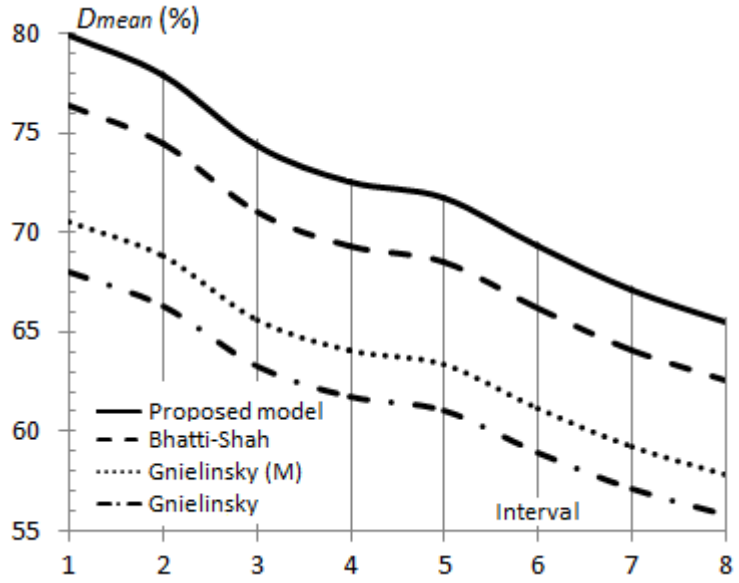

Figura 10. D_{mean} values in the correlation data (turbulent zone).

Figure 11 shows (with a 20 % error band) the adjustment obtained in the correlation of available experimental data with the model proposed in the present work, and provided by Equation (5).

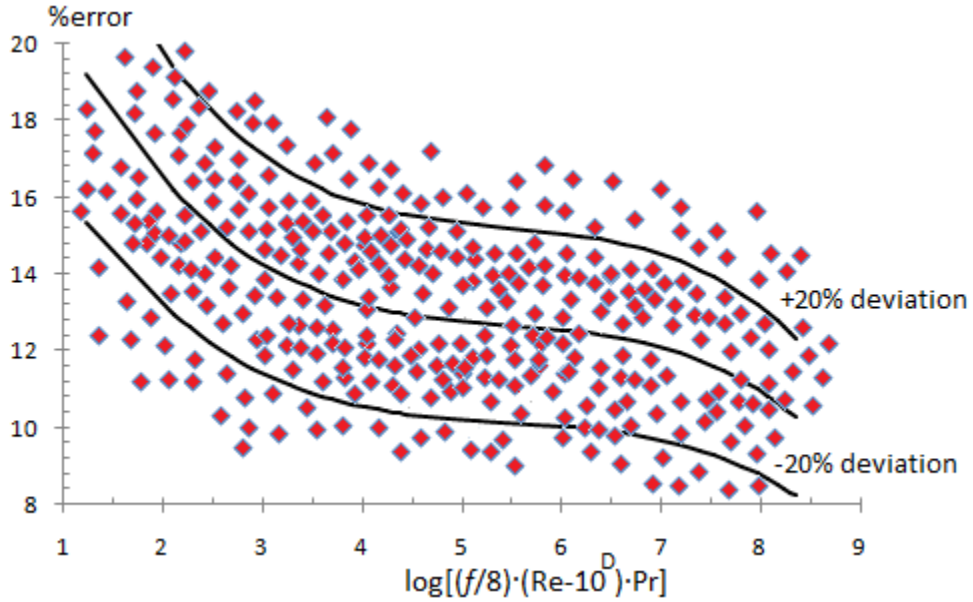

Figura 11. Correlation of Equation (5) with available experimental data.

4. CONCLUSIONS

- A new improved method for heat transfer calculation inside rough pipes has been proposed in the present work. The new correlation increases the validity range with respect to known models in the literature. The model presents a satisfactory agreement with the experimental data in each interval evaluated; therefore, can be considerate enough for use in practical applications. In available technical literature on the subject a model with similar characteristics is unknown.

- For the transition zone, 437 experimental data were used, verifying that the best adjustment was obtained by Equation (5), with a *MAE* value of 11.1 % for 84.5 % of the data and E_{max} of 16.9 % in the Interval 1, while for Interval 8, a *MAE* value equal to 16.6 % for 74.8 % of the data and E_{max} of 32.3 % are obtained. The more unfavorable indexes adjustment was achieved with Gnielinski's model with a *MAE* value of 23.2 % for 72.5 % of the data and E_{max} of 27.3 % in Interval 1, while for Interval 8, a *MAE* value equal to 32.8 % for 60.1 % of the data and E_{max} of 54.7 % are obtained. The modified correlation of Gnielinski can be used reservedly for heat transfer calculations in the transition regime, being preferable not to extend their use beyond Interval 1. The values obtained in the present study are slightly higher to the values commonly attributed to Bhatti-Shah's model.

- For the turbulent zone, 1 229 experimental data were used, verifying that the best adjustment was obtained by Equation (5), with a *MAE* value of 11.8 % for 80.2 % of the data and E_{max} of 17.3 % in Interval 1, while for Interval 8, a *MAE* value of 18.3 % for 70.4 % of the data and E_{max} of 34.1 % are obtained. The more unfavorable indexes adjustment was achieved with the Gnielinski's model with a *MAE* value of 23.9 % for 67.1 % of the data and E_{max} of 34.6 % in Interval 1, while for Interval 8, a *MAE* value of 36.6 % for 56.8 % of the data and E_{max} of 68.9 % are obtained, (however, it can be used for rapid estimations of the heat transfer coefficients in the turbulent zone). The values obtained in the present study are slightly higher to the values commonly attributed in the literature to the Bhatti-Shah's model.

- In this study, the models recognized in the literature as more precise (Bhatti-Shah and Gnielinski modified), showed a slightly larger uncertainty than the results obtained with the model proposed in the present work. Thus, Equation (5) is a better correlation, with a much better adjustment with the experimental data. Its use leads to a lower value of uncertainty in the calculation of the heat transfer coefficients in the turbulent and transitional regimes.

5. ACKNOWLEDGMENT

The authors are very grateful for the help provided by Professor S. Thomson, from the Department of Mathematics, Massachusetts Institute of Technology, USA.

6. REFERENCES

Ataei-Dadavi, I.; Chakkingal, M.; Kenjeres, S.; Kleijn, Ch. R. and Tummers, M. J. 2019: Flow and heat transfer measurements in natural convection

in coarse-grained porous media. *International Journal of Heat and Mass Transfer*, 130: 575-584.

Bhatti, M. S. and Shah, R. K. 1987: Turbulent and Transition Flow Convective Heat Transfer in Ducts. *Handbook of Single-Phase Convective Heat Transfer*. Kakac, S.; Shah, R. K. and Aung, W. (eds.) New York: Wiley-Interscience.

Bae, J. W.; Kim, W. K. and Chung, B. J. 2018: Visualization of natural convection heat transfer inside an inclined circular pipe. *International Communications in Heat and Mass Transfer*, 92: 15-22.

Bazán, F. S. V.; Bedin, L. and Bozzoli, F. 2016: Numerical estimation of convective heat transfer coefficient through linearization. *International Journal of Heat and Mass Transfer*, 102: 1230-1244.

Binu, T. V. and Jayanti, S. 2018: Heat transfer enhancement due to internal circulation within a rising fluid drop. *Thermal Science and Engineering Progress*, 8: 385-396.

Camaraza-Medina, Y.; Cruz-Fonticiella, O. M. and García-Morales, O. F. 2019: New model for heat transfer calculation during fluid flow in single phase inside pipes. *Thermal Science and Engineering Progress*, 11: 162-166.

Camaraza-Medina, Y.; Mortensen-Carlson, K.; Guha, P.; Rubio-González, A. M.; Cruz-Fonticiella, O. M. and García-Morales, O. F. 2019a: Suggested model for heat transfer calculation during fluid flow in single phase inside pipes (II). *International Journal of Heat and Technology*, 37(1): 257-266.

Camaraza-Medina, Y.; Sánchez-Escalona, A. A.; Cruz-Fonticiella, O. M.; García-Morales, O. F. 2019b: Method for heat transfer calculation on fluid flow in single-phase inside rough pipes. *Thermal Science and Engineering Progress*, 14: 100436.

Camaraza-Medina, Y.; Hernandez-Guerrero, A. and Luviano-Ortiz, J. L. 2020: Comparative study on heat transfer calculation in transition and turbulent flow regime inside tubes. *Latin American Applied Research*, 50(4): 309-314.

Camaraza-Medina, Y.; Hernandez-Guerrero, A.; Luviano-Ortiz, J. L. and Garcia-Morales, O. F. 2020: New improvement model for heat transfer calculation on viscous-gravitational fluid flow inside vertical and inclined tubes. *International Journal of Heat and Mass Transfer*, 159: 120108.

Cancan, Z.; Dingbiao, W.; Sa, X.; Yong, H. and Xu, P. 2017: Numerical investigation of heat transfer and pressure drop in helically coiled tube with spherical corrugation. *International Journal of Heat and Mass Transfer*, 113: 332-341.

Chen, Z. Y.; Cheng, M.; Liao, Q.; Ding, Y. D. and Zhang, J. N. 2019: Experimental investigation on the air-side flow and heat transfer

characteristics of 3-D finned tube bundle. *International Journal of Heat and* Mass Transfer, 131: 506-515.

Gnielinski, V. 2013: On heat transfer in tubes. *International Journal of Heat and Mass Transfer*, 63: 134-140.
DOI: http://dx.doi.org/10.1016/j.ijheatmasstransfer.2013.04.015

Huang, D.; Wu, Z.; Sunden, B. and Li, W. 2016: A brief review on convection heat transfer of fluids at supercritical pressures in tubes and the recent progress. *Applied Energy*, 162: 494-505.

Kumar, R.; Nadda, R.; Kumar, S.; Saboor, S.; Saleel, C. A.; Abbas, M. and Linul, E. 2023: Convective heat transfer enhancement using impingement jets in channels and tubes: A comprehensive review. *Alexandria Engineering Journal*, 70: 349-376.

Medina, Y. C.; Khandy, N. H.; Fonticiella, O. M. C. and Morales, O. F. G. 2017: Abstract of heat transfer coefficient modelation in single-phase systems inside pipes. *Mathematical Modelling of Engineering Problems*, 4(3): 126-131.

Medina, Y. C.; Fonticiella, O. M. C. and Morales, O. F. G. 2017: Design and modelation of piping systems by means of use friction factor in the transition turbulent zone. *Mathematical Modelling of Engineering Problems*, 4(4): 162-167.

Medina, Y. C.; Khandy, N. H.; Carlson, K. M.; Fonticiella, O. M. C. and Morales, O. F. C. 2018: Mathematical modeling of two-phase media heat transfer coefficient in air-cooled condenser systems. *International Journal of Heat and Technology,* 36(1): 319-324.

Mondal, S. and Field, R. W. 2018: Theoretical analysis of the viscosity correction factor for heat transfer in pipe flow. *Chemical Engineering Science*, 187: 27-32.

Petukhov, B. S. 1970: Heat transfer and friction in turbulent pipe flow with variable physical properties. *Advances in Heat Transfer*, 6: 503-564. DOI: https://doi.org/10.1016/S0065-2717(08)70153-9

Rabiee, R.; Desilets, M.; Proulx, P.; Ariana, M. and Julien, M. 2018: Determination of condensation heat transfer inside a horizontal smooth tube. *International Journal of Heat and Mass Transfer*, 124: 816-828.

Reis, M. C.; Sphaier, L. A.; Alves, L. S. and Cotta, R. M. 2018: Approximate analytical methodology for calculating friction factors in flow through polygonal cross section ducts. *Journal of the Brazilian Society of Mechanical Sciences and Engineering*, 40: 76.

Shankar, V. and Senadheera, S. 2024: Improved empirical convection heat transfer coefficient model to predict flexible pavement layer temperatures. *Construction and Building Materials*, 411: 134206.

Song, R.; Cui, M. and Liu, J. 2017: A correlation for heat transfer and flow friction characteristics of the offset strip fin heat exchanger. *International Journal of Heat and Mass Transfer*, 115: 695-705.

Thomas, J. A.; De Vincentis, B.; Janz, E. and Turner, B. 2024: A general approach for predicting convective heat transfer coefficients in turbulent systems. *International Journal of Heat and Mass Transfer*, 220: 124989.

Información adicional

Conflicto de intereses

Los autores declaran que no existen conflictos de intereses

Contribución de autores

YCM: búsqueda bibliografía sobre la temática, concepción general y ejecución de la investigación, así como la escritura y revisión del informe final. MM: ejecución de trabajos de investigación y procesamiento y presentación de resultados. YBG: análisis de los resultados, escritura y revisión del informe final.

ORCID

YCM, https://orcid.org/0000-0003-2287-7519

MM, https://orcid.org/0000-0002-3293-7573

YBG, https://orcid.org/0000-0001-5420-662

Received: 10/01/2024

Accepted: 04/02/2024